Electronic Supplementary Information for:

Soluble squaraine derivatives for 4.9% efficient organic photovoltaic cells

By Hisahiro Sasabe*[1,2], Tsukasa Igrashi[1], Yusuke Sasaki[1], Guo Chen,[2,3] Ziruo Hong[2,4], Junji Kido*[1,2]

[1]Department of Organic Device Engineering, Yamagata University, [2]Research Center for Organic Electronics 4-3-16 Jonan, Yonezawa, Yamagata 992-8510, Japan, [3]Key Laboratory of Advanced Display and System Applications, Ministry of Education, Shanghai University, Yanchang Road 149, Shanghai 200072, China, [4]Department of Materials Science and Engineering, University of California, Los Angeles, Los Angeles, CA 90095, USA.

General Procedures. ^{1}H NMR spectra were recorded on JEOL 400 (400 MHz) spectrometer. Mass spectra were obtained using a JEOL JMS-K9 mass spectrometer. Differential scanning calorimetry (DSC) was performed using a Perkin-Elmer Diamond DSC Pyris instrument under nitrogen atmosphere at a heating rate of 10°C min^{-1}. Thermogravimetric analysis (TGA) was undertaken using a SEIKO EXSTAR 6000 TG/DTA 6200 unit under nitrogen atmosphere at a heating rate of 10°C min^{-1}. Ultraviolet–visible (UV–vis) absorption spectra were collected using a UV–vis–NIR spectrophotometer (SHIMADZU, UV-3150). Photoluminescence (PL) spectra were measured using a FluroMax-4 (Horiba-Jobin-Yvon) luminescence spectrometer. The concentration of the solutions for UV–vis absorption and PL measurements was 1×10^{-6} M in chloroform. Thin films for UV–vis absorption and PL measurements were prepared by spin coating a chloroform solution onto quartz substrates. Cyclic voltammetry (CV) measurements were performed using a PC controlled ALS/CHI 660B electrochemical workstation in an N_2-filled glove box. The experiments were conducted in 0.5 mM dichloromethane (CH_2Cl_2) solution of SQ with 0.13 M tetrabutylammonium tetrafluoroborate ($TBABF_4$, as supporting electrolyte) at a scan rate of 0.1 V/s using a glassy carbon electrode as the working electrode, platinum wire as the counter electrode, and a Ag/Ag^+ electrode as the reference electrode. Ferrocene was used as an internal standard. The electrochemical potential was internally calibrated against the standard ferrocene/ferrocenium (Fc/Fc^+) redox couple (with an absolute energy of –4.8 eV vs. vacuum). On the basis of the oxidation potential onset (E_{ox}) and the reduction potential onset (E_{red}) referenced to the Fc/Fc^+ internal standard, the HOMO and lowest unoccupied molecular orbital (LUMO) were calculated according to the equations HOMO = –(E_{ox} + 4.8) (eV) and LUMO = –(E_{red} + 4.8) (eV), where E_{ox} and E_{red} are the oxidation potential onset and the reduction potential onset, respectively, vs. Fe/Fe^+. The energy band gap (E_g^{ec}) was calculated according to the equation E_g^{ec} = LUMO – HOMO.

Device fabrication and characterization: Patterned ITO-coated glass substrates were sequentially cleaned using detergent, deionized water, acetone, and isopropanol in an ultrasonic bath. The cleaned substrates were dried in an oven at 80 °C for 12 h before use. Substrates were exposed to UV ozone for 20 min, and were then immediately transferred into a high-vacuum chamber for the deposition of 6-nm MoO_3 at a base pressure of 1×10^{-5} Pa. Photoactive layers (thickness: 70 ± 5 nm) were fabricated by spin-coating SQ:$PC_{71}BM$ solution (20 mg/ml in chloroform) onto a MoO_3-coated ITO surface in a N_2-filled glove box. Finally, the substrates were transferred back to the high-vacuum chamber, where BCP (10 nm) and Al (100 nm) were deposited as the top electrode, resulting in a final OPV cell with the structure ITO/MoO_3 (6 nm)/SQ:$PC_{71}BM$ (70 nm)/BCP (10 nm)/Al (100 nm). The active area of the OPV cells was 0.09 cm^2, as defined by the overlap of the ITO anode and Al cathode. Current density–voltage (J–V) and external quantum efficiency (EQE) characterizations of OPV cells were performed on a CEP-2000 integrated system manufactured by Bunkoukeiki Co. The integration of EQE data over a AM1.5G solar spectrum yielded calculated J_{sc} values with an experimental variation of less than 3% relative to the J_{sc} measured under 100-mW/cm^2-simulated AM1.5G light illumination.

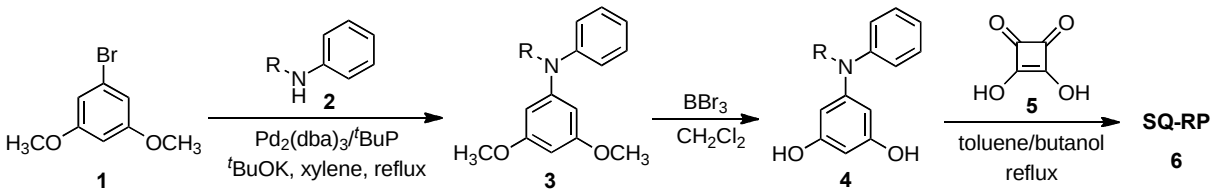

Scheme 1. Synthesis of SQ-RP

Synthetic route of SQs is shown in **Scheme 1**. The precursor **4** was prepared via a Buchwald-Hartwig amination reaction of bromide **1** with alkylaniline **2** followed by a demethylation reaction of **3**. Then, a condensation reaction between amine **4** and squaric acid **5** gave the target SQ-RP **6** in 82–88% yield.

Synthesis of SQ-BP. A mixture of aniline precursor (1.64 g, 6.38 mmol), squaric acid (0.36 g, 3.20 mmol), 1-butanol (15 mL), and toluene (45 mL) was stirred for 16 hours at reflux temperature under N_2 flow with azeotropic distillation of water. After the mixture was concentrated to ca. 10 mL, cyclohexane (30 mL) was added to the reaction mixture. Then, the solvent was cooled to room temperature. The precipitate was filtered, and washed with methanol and hexanes, dried in vacuo to afford SQ-BP as green microcrystals. The compound was

further purified by recrystallization using cyclohexane-toluene (1.78 g, 88%). The purity of SQ was confirmed by HPLC analysis using THF–methanol (1 : 4) as eluents.

SQ-BP: ^{1}H NMR (400 MHz, $CDCl_3$): δ 10.97 (s, 4H), 7.45 (dd, 4H, *J*=7.7, 7.7 Hz), 7.36 (t, 2H, *J*=7.5 Hz), 7.18 (d, 4H, *J*=7.7 Hz), 5.70 (s, 4H), 3.69 (t, 4H, *J*=7.9 Hz), 1.72–1.64 (m, 4H), 1.38–1.29 (m, 4H), 0.92 (t, 6H, *J*=7.3 Hz) ppm; MS: *m/z* 593 $[M]^+$; Anal. Calcd for $C_{36}H_{36}N_2O_6$: C, 72.95; H, 6.12; N, 4.73%. Found: C, 72.99; H, 6.11; N, 4.66%.

SQ-OP: SQ-OP was synthesized by the same procedure using the corresponding aniline precursor. Yield: 83%. ^{1}H NMR (400 MHz, $CDCl_3$): δ 10.96 (s, 4H), 7.45 (dd, 4H, *J*=7.7, 7.7 Hz), 7.36 (t, 2H, *J*=7.5 Hz), 7.17 (d, 4H, *J*=7.7 Hz), 5.70 (s, 4H), 3.68 (t, 4H, *J*=8.0 Hz), 1.72–1.65 (m, 4H), 1.30–1.23 (m, 20H), 0.87 (t, 6H, *J*=6.9 Hz) ppm; MS: *m/z* 706 $[M]^+$; Anal. Calcd for $C_{44}H_{52}N_2O_6$: C, 74.79; H, 7.44; N, 3.97%. Found: C, 75.24; H, 7.68; N, 3.89%.

SQ-DP: SQ-DP was synthesized by the same procedure using the corresponding aniline precursor. Yield: 82%. ^{1}H NMR (400 MHz, $CDCl_3$): δ 10.97 (s, 4H), 7.45 (dd, 4H, *J*=7.7, 7.7 Hz), 7.36 (t, 2H, *J*=7.5 Hz), 7.17 (d, 4H, *J*=7.7 Hz), 5.69 (s, 4H), 3.68 (t, 4H, *J*=7.9 Hz), 1.72–1.64(m, 4H), 1.31–1.24 (m, 36H), 0.88 (t, 6H, *J*=7.0 Hz) ppm; MS: *m/z* 818 $[M]^+$; Anal. Calcd for $C_{52}H_{68}N_2O_6$: C, 76.44; H, 8.39; N, 3.43%. Found: C, 76.44; H, 8.66; N, 3.35%.

Table S1. Solubility of SQ-RP derivatives.

Compound	$CHCl_3$	Toluene	THF	1,4-dioxane
SQ-MP	< 1 mg/ml	< 1 mg/ml	< 1 mg/ml	< 1 mg/ml
SQ-BP	**> 8 mg/ml**	< 1 mg/ml	< 1 mg/ml	< 1 mg/ml
SQ-OP	**> 10 mg/ml**	≒1 mg/ml	≒1 mg/ml	< 1 mg/ml
SQ-DP	**> 16 mg/ml**	**> 16 mg/ml**	**> 16 mg/ml**	< 1 mg/ml

Table S2. Physical properties of SQ-RP derivatives.

Compound	solution in $CHCl_3$[a]		thin film[b]	T_g[c]/T_m[d]/T_d[d] (℃)	HOMO/LUMO[e] (eV)
	ε (10^5 $M^{-1}cm^{-1}$)	λ_{max} (nm)	λ_{max} (nm)		
SQ-MP	3.2	645	n.d.[f]	n.d. / n.d. / 321	n.d.[g]
SQ-BP	3.6	650	697	n.d. / n.d. / 322	5.3 / 3.6
SQ-OP	3.5	650	694	n.d. / 230 / 290	5.3 / 3.6
SQ-DP	3.5	650	581, 673	n.d. / 177 / 298	5.3 / 3.6

a) Absorption and emission spectra were measured in $CHCl_3$ (10^{-6} M). b) Thin film was formed from 3 mg/ml $CHCl_3$ solution on a quartz substrate. c) Measured by a DSC. d) Measured by a TGA. e) Measured by a CV (0.5 mM in CH_2Cl_2). f) Solubility is too low to form uniform thin solid film. g) Solubility is too low to measure.

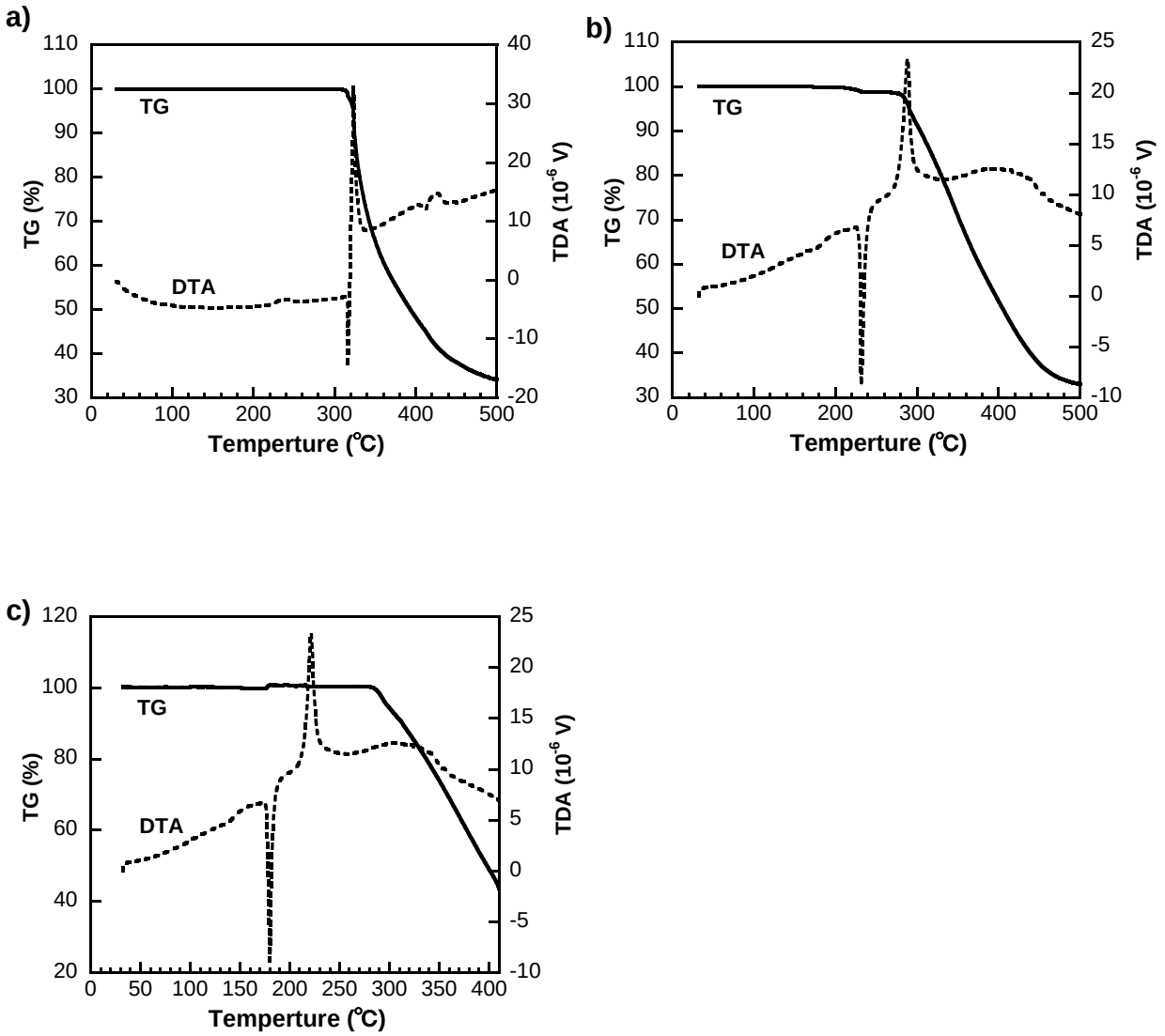

Fig. S1. DTA-TG curves of a) SQ-BP, b) SQ-OP, c) SQ-DP.

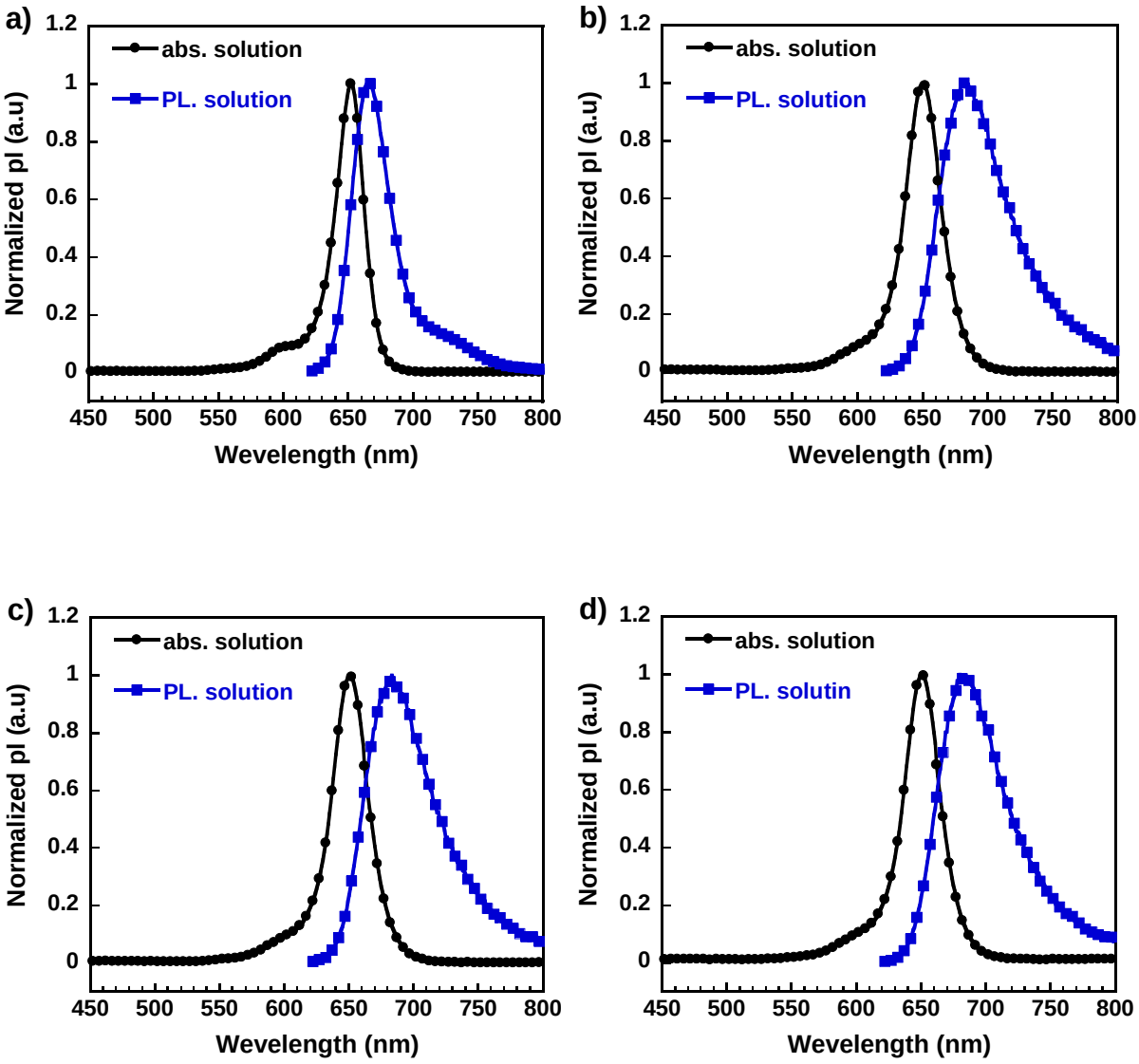

Fig. S2. UV-vis absorption and photoluminescence (PL) of a) DIB-SQ, b) SQ-BP, c) SQ-OP, d) SQ-DP in $CHCl_3$ (10^{-6} M).

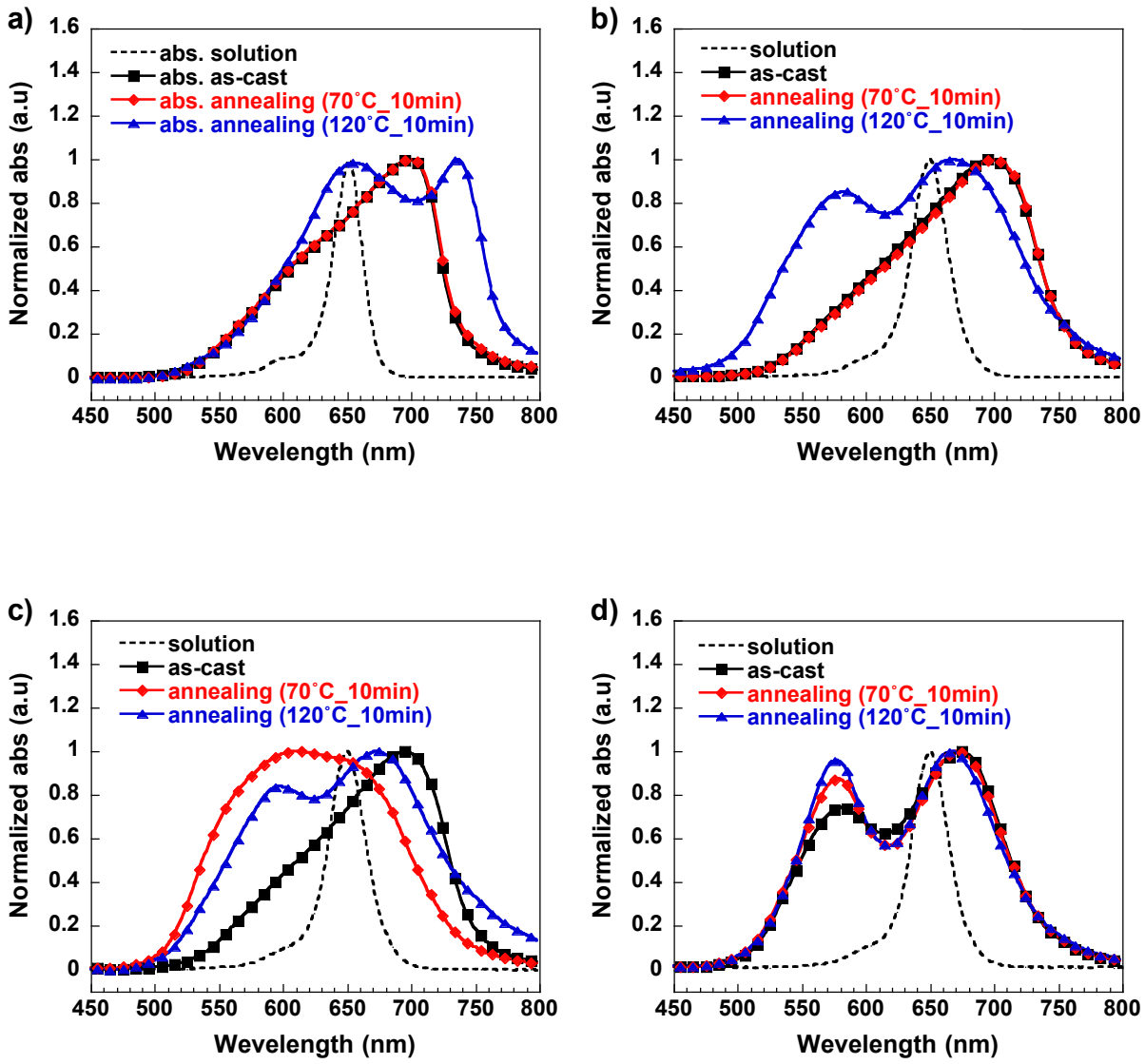

Fig. S3. UV-vis absorption and photoluminescence (PL) spectra of a) DIB-SQ, b) SQ-BP, c) SQ-OP, d) SQ-DP as 20 nm thin film on quartz substrate.

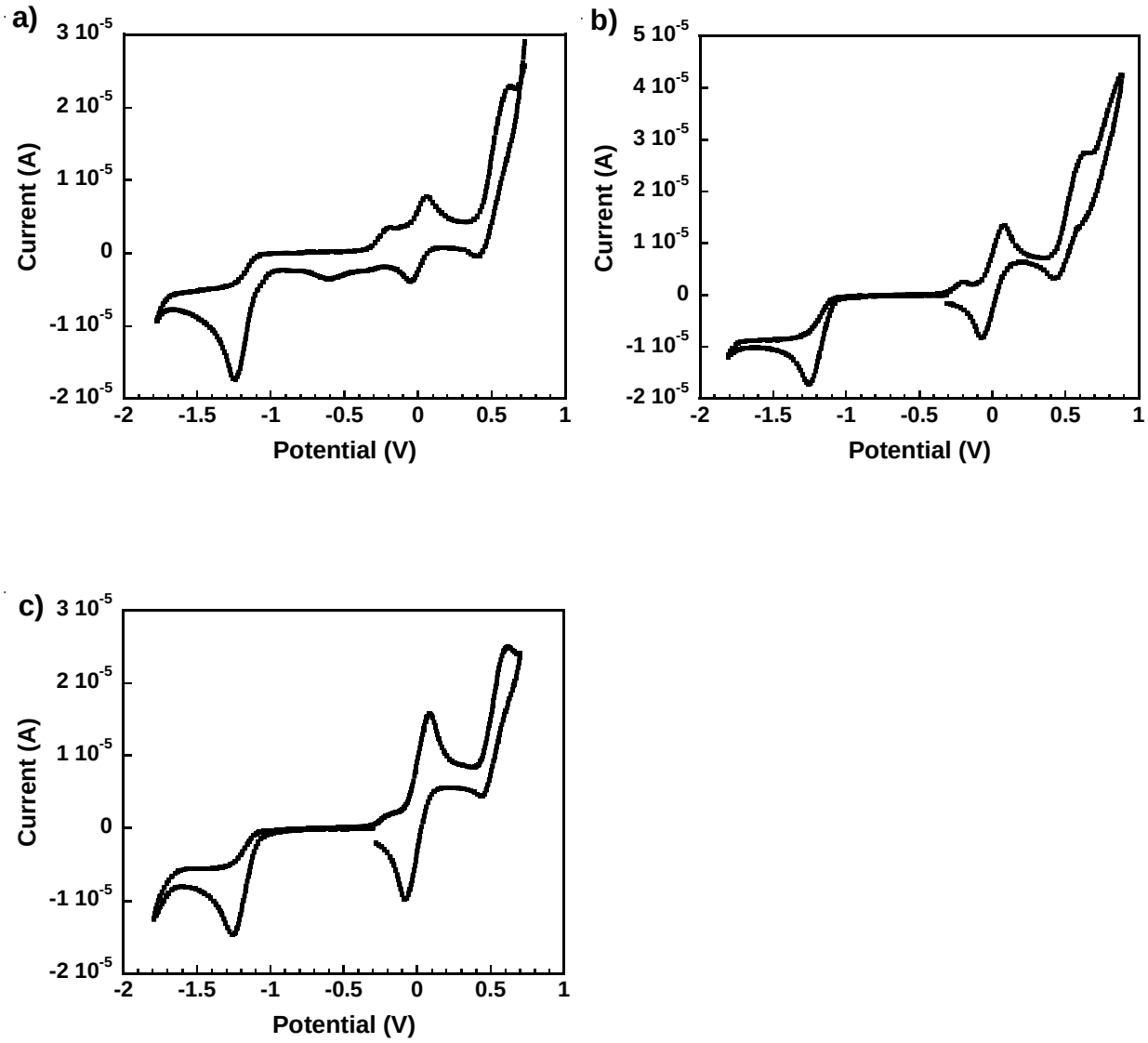

Fig. S4. Cyclic voltammetry (CV) of SQ-RP in CH_2Cl_2 solution with 0.13 M $TBABF_4$ using ferrocene/ferrocenium redox couple (Fc/Fc^+). a) SQ-BP, b) SQ-OP, c) SQ-DP.

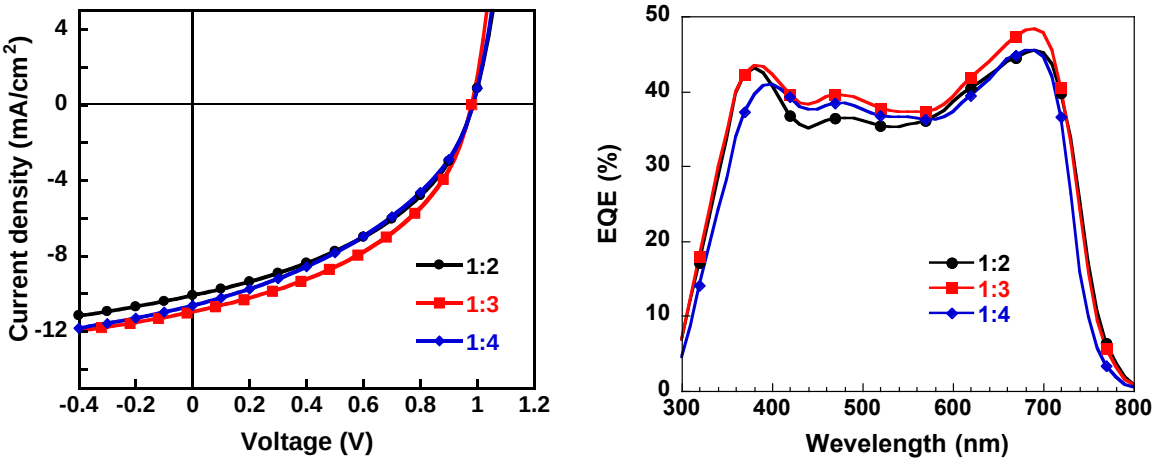

Fig. S5. *J–V* curves illuminated under AM 1.5 G solar spectrum at 100 mW/cm^2 illumination and EQE spectra of SQ-BP:PC_{70}BM-based devices with various SQ-BP:PC_{70}BM weight ratios.

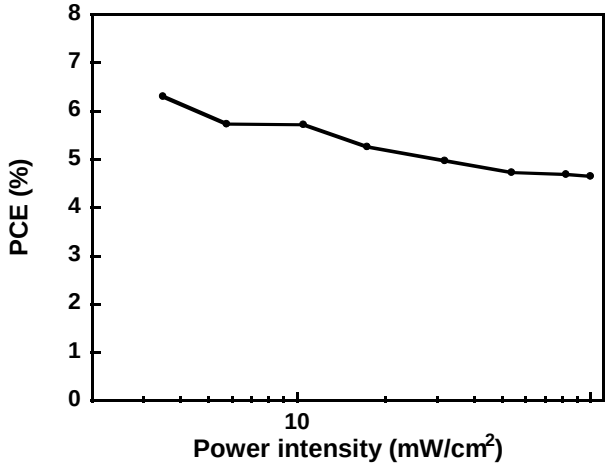

Fig. S6. PCE of SQ-BP:PC_{70}BM=1:3-based device versus power intensity.

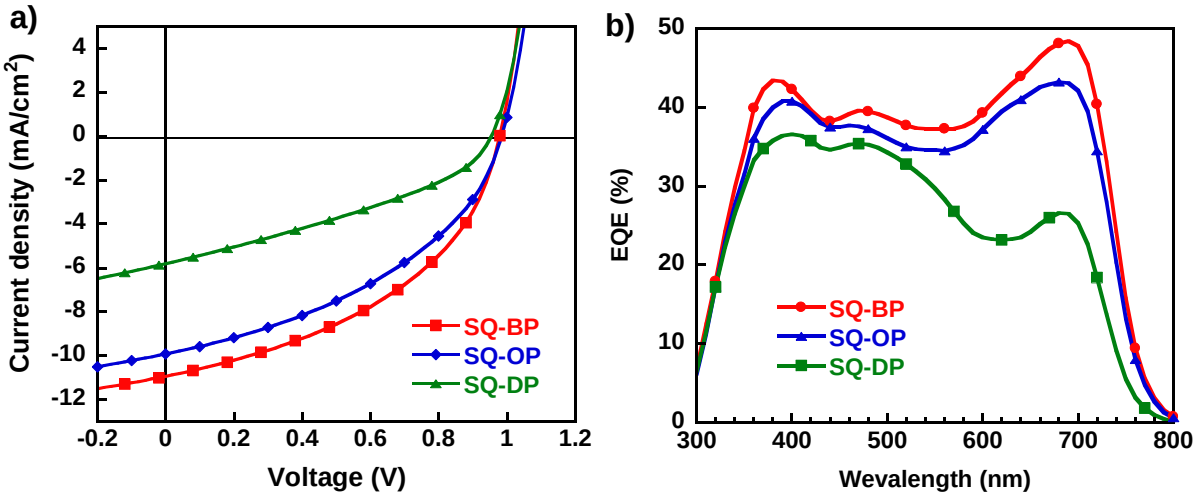

Fig. S7. (a) *J–V* curves illuminated under AM 1.5 G solar spectrum at 100 mW/cm^2 illumination; and (b) EQE spectra of SQ-RP:PC_{70}BM=1:3-based device.

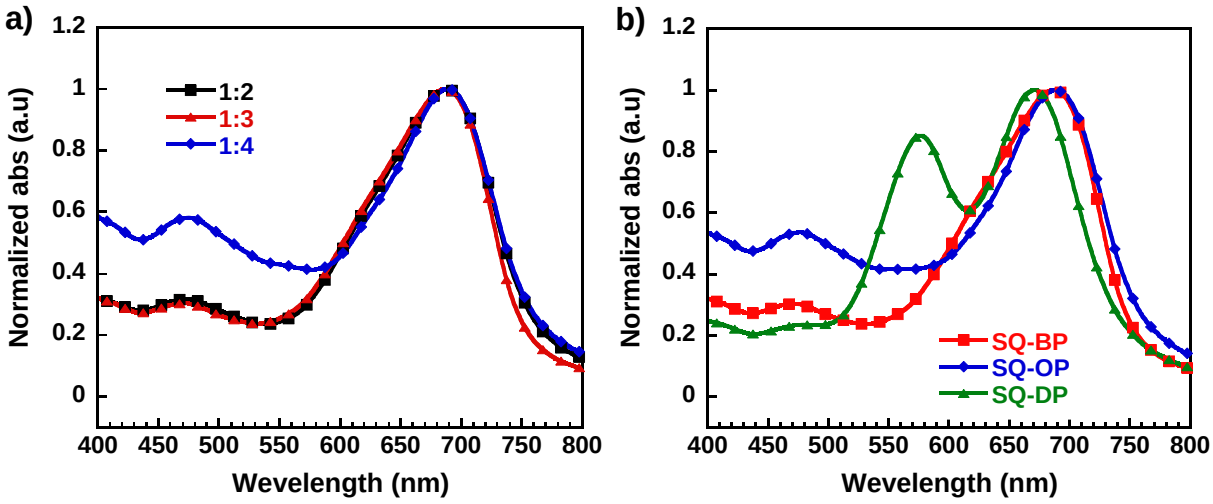

Fig. S8. UV-vis spectra of active layers with a) SQ-BP:$PC_{70}BM$, b) SQ-RP:$PC_{70}BM$ = 1:3.

Table S3. Key OPV parameters of SQ-based devices based on various SQ:$PC_{71}BM$ weight ratios.

Compound	weight ratio	Voc (V)	Jsc (mA/cm2)	FF	PCE (%)
SQ-BP	1 : 2	0.98 (0.98)	10.40 (10.27)	0.43 (0.43)	4.37 (4.29)
	1 : 3	0.98 (0.98)	11.01 (10.99)	0.45 (0.45)	4.86 (4.76)
	1 : 4	0.98 (0.98)	10.61 (10.91)	0.41 (0.40)	4.29 (4.19)
SQ-OP	1 : 3	0.99 (0.99)	9.96 (9.86)	0.41 (0.41)	4.08 (4.05)
SQ-DP	1 : 3	0.96 (0.96)	5.72 (5.75)	0.36 (0.35)	1.97 (1.93)

Average values of 8 devices are shown in parentheses.